THE ROLE OF OLIVINE IN FE-CARBONATE FORMATION IN GALE CRATER, MARS. S.M.R. Turner[1*], S.P. Schwenzer[1**], J.C. Bridges[2], B. Sutter[3], M.T. Thorpe[3], E.B. Rampe[4], and A.C. McAdam[5]. [1]AstrobiologyOU, STEM Faculty, The Open University, UK, (*stuart.turner@open.ac.uk, **susanne.schwenzer@open.ac.uk). [2]School of Physics and Astronomy, University of Leicester, UK. [3]Jacobs, NASA JSC, USA. [4]NASA JSC, USA. [5]NASA Goddard Space Flight Center, USA.

Introduction: Carbonates have been identified in remote sensing datasets [1,2], martian meteorites [3,4], and in-situ with rovers at Gale [5] and Jezero [6] craters. In Gale crater, traces of carbonate have been found by the SAM instrument throughout the Mars Science Laboratory mission, e.g., at Rocknest [7] and Pahrump Hills [8], with models for carbonate formation at Pahrump Hills explored by [9]. Further up-section, CheMin data of clay-rich Glen Torridon (GT) samples show that five out of seven drill samples from GT contain Fe-carbonate alongside phyllosilicates [5]. The GT sediments were deposited in a lacustrine environment and subsequently underwent multiple episodes of diagenesis [5,10,11].

In this work, we explore the role of olivine in the formation of carbonates by modelling the interaction of different martian olivines with a previously modeled Gale groundwater. We then explore the incongruent dissolution of host rocks within the GT sediments by mixing olivine with quantities of the Kilmarie drill sample chemical composition as the reactant rock.

Modeling Method: CHIM-XPT, a program for computing multicomponent heterogeneous chemical equilibria in aqueous-mineral gas systems, calculates equilibrium for each water / rock reaction step between a user-defined fluid and dissolved chemical reactant list (the rock) [12]. Here we focus on 10-1000000 W/R, utilizing the low-temperature BRGM Thermoddem thermochemical database [13].

The Starting Fluid. We utilize the model Gale groundwater, "Gale Portage Water" (GPW) [14,15]. The solution is initially oxidizing and was adapted by equilibration with an atmosphere of Noachian/Early Hesperian Mars (~1 bar [16]) partial pressure (pCO_2), resulting in 5.2×10^{-2} moles/kg HCO_3^-.

The Reactant Rock. We used a variety of chemical compositions representative of olivines found in the Martian meteorites and Gale crater. These included olivines from shergottites (Los Angeles (Fa94 and Fa89 [17]), DaG476 (Fo77) and Y98 (Fo84) [18]), a nakhlite (Lafayette Fo33 [19]), and Gale crater (Rocknest, Fo57 [20]).

To explore the preferential dissolution of olivine within the Gale sediments, the Kilmarie sample was selected to mix with Rocknest olivine. Kilmarie, from GT, had minimal diagenetic overprint with diagenetic features limited to cross-cutting Ca-sulfate veins [10] and minor amounts of general discoloration and pitting [11]. As Ca-sulfates are attributed to a later phase of alteration than is of interest in this abstract [21], 11% $CaSO_4$ was removed from the APXS measurement, which was used as the reactant rock composition in the modelling with 10% Fe^{3+}/Fe_{total}. Three mixes were devised. Mix 1 was 100% Kilmarie, Mix 2 was 50% Kilmarie and 50% Rocknest olivine, and Mix 3 was 10% Kilmarie and 90% Rocknest olivine.

Modeling Results: Fig. 1 summarizes the secondary alteration assemblages for six pure olivines reacted with GPW. Carbonate formation dominates the secondary assemblage at 1000 W/R, with quartz dominating at 10000 W/R. At 100 W/R, carbonates form alongside hematite and serpentines. As demonstrated by Fig. 1, the type of carbonate that forms can be directly related to the type of olivine present within the reactant rock. Fa94 olivine forms 77 wt.% siderite at 1000 W/R, which decreases to 34 wt.% siderite and 1 wt.% ankerite at 100 W/R. Due to the low Mg content of the olivine only 2.6 wt.% magnesite forms at 100 W/R. Conversely, Fo84 olivine forms considerably more Mg-carbonate. At 1000 W/R 48 wt.% magnesite forms with 19 wt.% siderite, and at 100 W/R 30 wt.% magnesite forms with 0.5 wt.% dolomite. Rocknest olivine forms 53 wt.% siderite alongside 15 wt.% magnesite at 1000 W/R, whereas at 100 W/R 30 wt.% magnesite forms with 0.01 wt.% dolomite.

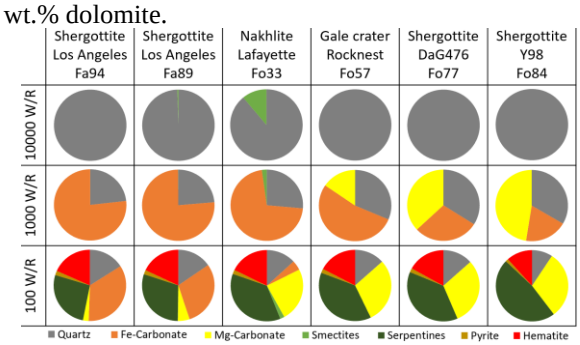

Fig. 1. Secondary mineral assemblage phase wt.% of olivines reacted with high-CO_2 GPW at 10,000, 1,000, and 100 W/R. Models were run with CHIM-XPT at 50 °C.

Fig. 2 shows the reaction of Kilmarie bulk with GPW results in Fe-carbonate dominating the carbonate phases from 3333 W/R to 28 W/R, with Fe-carbonate constituting 31 wt.% of the secondary assemblage at 345 W/R. Both Mg-carbonate and Ca-carbonate constitute ~9 wt.% at 100 and 26 W/R, respectively. Mixes 2 and 3 explore the preferred dissolution of olivine within the Kilmarie sample by including 50% and 90% Rocknest olivine, respectively. In the presence of 50% olivine, Fe-carbonate dominates the carbonate phases from 5000 W/R to 170 W/R, peaking at 1100

W/R with 43 wt.%. Considerably more Mg-carbonate forms than in pure Kilmarie composition, peaking at 26 wt.% at 140 W/R. with only ~2.7 wt.% Ca-carbonate forming at 10 W/R. Almost pure olivine with 10% of bulk Kilmarie composition, as shown in Fig. 2, has Fe-carbonate dominating from 10000 W/R to 290 W/R, peaking at 1700 W/R with 58 wt.%. Mg-carbonate dominates from 290 W/R to 10 W/R, with no Ca-carbonate phase forming.

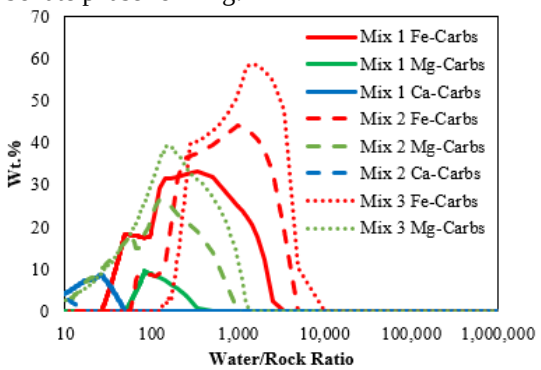

Fig. 2. CHIM-XPT modelled carbonates from reacting mixes 1-3 with CO_2-rich GPW at 50 °C. Summed Fe-carbonates include siderite and ankerite, Mg-carbonates include magnesite and dolomite, and Ca-carbonates is calcite.

Fig. 3 shows the type of Fe-carbonate present in the secondary mineral assemblages. Siderite tends to form 10000 – 100 W/R, with ankerite forming from 1000 – 30 W/R. The transition point from siderite to ankerite being dominant is at 220 W/R.

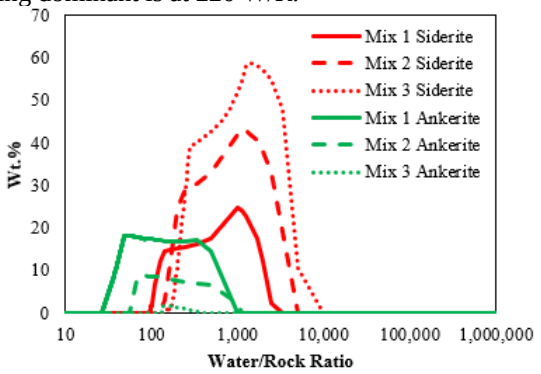

Fig. 3. CHIM-XPT modelled Fe-carbonates from reacting mixes 1-3 with CO_2-rich GPW at 50 °C.

Discussion: Given the detections of Fe-carbonate in Gale, we focus on those in our models, and this initially helps to constrain the W/R ratios at which those phases formed in Gale: for siderite bearing sediments a W/R ratio of 1000 – 10000 is likely, as also shown by [22], unless there is also evidence for ankerite and magnesite at which point lower W/R ratios could be considered. A caveat being the availability of Ca within the models, as this is going to directly affect the amount of ankerite that could form, as demonstrated by Fig. 3. However, it is important to note that other thermochemical modelling studies have actively suppressed magnesite because it is kinetically retarded in favor of alternative Mg-carbonates [23].

The modelled fluid for Rocknest olivine (Fig. 1) showed peak concentrations of Mg at 1250 W/R of 4.9 × 10^{-3} moles/kg, with a pH of 5.6. At this point the secondary assemblage has 60 wt.% siderite. The role of Mg in a second or later diagenetic stage is of interest, due to the presence of Mg-sulfates in Gale.

Understanding the carbon cycle on Mars requires comparison to other carbonate bearing environments, such as Jezero crater. Data returned by the Perseverance rover has indicated the presence of carbonates within both the Séítah and Máaz formations [24]. Fo55 olivine and Fe,Mg-carbonate accompanied by Mg,Ca-sulfate within the Séítah formation [6] is comparable to Rocknest olivine mixes modelled in this abstract. The high concentration of Mg in the modelled Rocknest fluid raises the question of fluid-fluid mixing with SO_4-rich fluids to produce Mg-sulfates at Gale and Jezero.

Summary: The modelling presented here demonstrates the importance of the role of olivine and GT host rock in the formation of siderite and ankerite. Given the trace detections of ankerite in the GT samples [5], the proportions of olivine to host rock represented by Mixes 2 and 3 in Figs. 2 and 3 suggest the potential for the preferred dissolution of olivine, which has been previously explored in Gale crater by [14].

Our results presented here further reinforce previous modelling [15] that a two-step process is necessary to form the carbonate-bearing assemblage present in Gale crater. This raises the question as to whether the carbonate formation process in the nakhlite martian meteorites [25] are analogous to the carbonate formation process in Gale crater, as those are controlled by olivine-dominated dissolution and subsequent patchy replacement of carbonate by clay [3,4,25].

References: [1] Ehlmann and Edwards, 2014. *Annual Rev. 42*, 291-315. [2] Horgan et al., 2020. *Icarus 339*, 113526. [3] Bridges et al., 2019. Carbonates on Mars in 'Volatiles on Mars'. 1st edition. Elsevier. [4] Piercy et al., 2022. *GCA 326*, 97-118. [5] Thorpe et al., 2022. *JGR: Planets 127*(11), e2021JE007099. [6] Tice et al., 2022. *Science Advances 8*(47) eabp9084. [7] Archer Jr et al., 2014. *JGR: Planets 119*(1), 237-254. [8] Sutter et al., 2017. *JGR: Planets 122*(12), 2574-2609. [9] Schieber et al., 2022. *Sedimentology 69*(6), 2371-2435. [10] Gasda et al., 2022. *JGR: Planets*, e2021JE007097. [11] Rudolph et al., 2022. *JGR: Planets*, *127*(10), e2021JE007098. [12] Reed 1998. *Rev. Econ Geol. 10*, 109-124. [13] Blanc et al., 2012. *Applied Geochemistry 27*(10), 2107-2116. [14] Bridges et al., 2015. *JGR: Planets 120*(1), 1-19. [15] Turner et al., 2022. LPSC abs #2167. [16] Craddock and Greeley, 2009. *Icarus 204*(2), 512-526. [17] Warren et al., 2004. *MaPS 39*, 137-156. [18] Shearer et al., 2008. *MaPS 43*, 1241-1258. [19] Treiman, 2005. *Geochemistry 65*(3), 203-270. [20] Morrison et al., 2018. *Am Min 103*(6), 857-871. [21] Bristow et al., 2021. *Science 373*(6551). [22] Kite and Melwani Daswani, 2019. *EPSL 524*, 115718. [23] Melwani Daswani et al., 2016. *MaPS 51*(11), 2154-2174. [24] Clavé et al., 2022. *JGR: Planets*, e2022JE007463. [25] Bridges and Schwenzer, 2012. *EPSL 359*, 117-123.